Temporal fluctuation of singular values caused by dynamical noise in chaos

Masaru Todoriki,* Hiroyuki Nagayoshi, and Atsuyuki Suzuki
Department of Quantum Engineering and Systems Science, The University of Tokyo, 7-3-1 Hongo, Bunkyo-ku, Tokyo 113-8656, Japan
(Received 22 February 2005; published 9 September 2005)

We propose a method to evaluate the influence of dynamical noise on chaotic systems. For Chua's electronic circuit as a typical chaotic system, it is demonstrated that dynamical noise influences the temporal fluctuation of singular values obtained from singular value decomposition. This behavior, however, is independent of additional measurement noise. The appearance of this fluctuation is compared to *Shannon entropy* of coarse-grained trajectories in its dependence on the noise amplitude. Additionally, noise-induced stabilization is discussed from the change of a pattern of a flip-flop process.

DOI: 10.1103/PhysRevE.72.036207 PACS number(s): 05.45.−a, 05.40.−a, 43.50.+y, 74.40.+k

I. INTRODUCTION

Every physical system is subject to noise in the real world. In general, there are two types of noise in any physical system, namely, measurement noise and dynamical noise. Different from the former, the latter type of noise is said to be realistically intrinsic to a physical system and yields an extremely complicated mechanism accompanied by feedback. As a result, it is quite difficult to analyze on both the theoretical and experimental levels. On the other hand, since a chaos system displays particularly strong nonlinearity and sensitivity to its initial condition, dynamical noise may have a remarkable and fatal influence on a chaos system. Numerous studies concerning dynamical noise in chaos have appeared. Although recently some studies estimated noise levels by means of the Bayesian approach [1–3], a target noise type is restricted to the additive one with a Gaussian probability distribution. Therefore, it is difficult to apply those methods to some general situations. In addition, dynamical noise brings about stabilization of the system such as stochastic resonance [4,5], vibrational resonance [6–8], coherence resonance [9–11], and noise-induced stabilization [10,12–16]. Accordingly, we try to show numerically a method to evaluate the influence of dynamical noise on chaos independently of noise types and to qualitatively distinguish it from that of measurement noise. Furthermore, noise-induced stabilization is also discussed. As an analytical tool, singular value decomposition (SVD), which is frequently employed for a principal component analysis [17,18], is used for inquiring into the temporal fluctuation of a chaotic system caused by noise. Empirically, singular values are obtained from SVD and *the temporal fluctuation of singular values (TFSV)* is investigated.

II. TEMPORAL FLUCTUATION OF SINGULAR VALUES (TFSV)

Generally, dynamical noise and measurement noise are defined for a flow system, respectively, as follows:

$$\dot{\mathbf{x}} = \mathbf{f}(\mathbf{x}, \xi^{(\mathbf{D})}), \tag{1a}$$

$$\mathbf{y} = \mathbf{g}(\mathbf{x}) + \xi^{(\mathbf{M})}, \tag{1b}$$

where $\mathbf{x}$ and $\mathbf{y}$ are, respectively, the underlying state vector and the observed one; $\mathbf{f}$ is a governing function of the system; $\mathbf{g}$ is an observation function; and $\xi^{(\mathbf{D})}$ and $\xi^{(\mathbf{M})}$ are dynamical and measurement noise, respectively.

SVD is the operation to diagonalize the singular matrix. Now, if the $N\times n$ rectangular matrix X is diagonalized, the covariance matrix X^tX can be decomposed into $X^tX=V\Sigma^2V^t$, where Σ^2 is the $n\times n$ diagonal matrix and V and V^t are the $n\times n$ orthogonal matrix and the transposed matrix of V, respectively. Here, $VV^t=V^tV=I_n$ is satisfied using the $n\times n$ unit matrix I_n. As $\Sigma^2=\mathrm{diag}[\sigma^2(1),\sigma^2(2),\ldots,\sigma^2(n)]$ is obtained, we can extract singular values (*SV*s) $\{\sigma(i)|i=1,2,\ldots,n\}$, which are nonzero. The relatively larger SVs correspond to the principal orthogonal basis of the deterministic system. The smaller SVs correspond to the nondeterministic components, which are mainly influenced by numerical error. However, the effect of the rounding error is not presently examined, as it is extremely difficult to consider such errors in the analysis. In general, measured data are frequently obtained as a scalar time series, so the procedure of SVD is explained for such data. Now, an (n,J) window $\{v_i,v_{i+J},\ldots,v_{i+(n-1)J}\}$ is prepared, where n is the number of elements of the window and J is a sample time in applying the method of delays as described in Ref. [17]. Here, a finite measured time series $\{v_i\in R|i=1,2,\ldots,N+n-1\}$ is transformed into the $N\times n(N\gg n)$ matrix X and, thus, the $n\times n$ covariance matrix X^tX can be expressed as follows:

$$X^tX=\begin{pmatrix} \langle v_i^2\rangle & \langle v_iv_{i+J}\rangle & \cdots & \langle v_iv_{i+(n-1)J}\rangle \\ \langle v_{i+J}v_i\rangle & \langle v_{i+J}^2\rangle & \cdots & \langle v_{i+J}v_{i+(n-J)J}\rangle \\ \vdots & \vdots & \ddots & \vdots \\ \langle v_{i+(n-1)J}v_i\rangle & \langle v_{i+(n-1)J}v_{i+J}\rangle & \cdots & \langle v_{i+(n-1)J}^2\rangle \end{pmatrix}, \tag{2}$$

where $\langle\cdot\rangle$ denotes the time average for $i=1,2,\ldots,N$. The appearance that noise influences SVs can be explained by considering the behavior of each component of X^tX indicated in Eq. (2).

*Electronic address: todoriki@q.t.u-tokyo.ac.jp

A. Measurement noise

In the presence of measurement noise, each SV uniformly increases, since the underlying state vectors and the noise are uncorrelated, as explained in Ref. [17]. Namely, the covariance matrix X^tX has a quite simple structure that is almost diagonal, where all diagonal values are larger by the same amount than those of a noiseless case. If the system remains steady, such diagonal values are expected to be nearly constant independent of the passage of time.

B. Dynamical noise

On the other hand, in the presence of dynamical noise, the result is utterly different from the case of measurement noise, and X^tX loses its simple structure. Since the underlying state vectors and dynamical noise are correlated, the dynamical noise complicatedly affects both each diagonal component $A_i=\langle v_i^2\rangle$ and each off-diagonal component $B_{i,j}=\langle v_i v_j\rangle (i\neq j)$ of X^tX $(i,j=1,2,\ldots,n)$. The operation of SVD is to reduce the values of all of $B_{i,j}$ by means of a similarity transformation of the orthogonal matrix. Accordingly, when each value of $B_{i,j}$ is reduced in the process of SVD, the complexity of each $B_{i,j}$ spreads on each A_i and, therefore, each value of A_i complicatedly changes. Moreover, since the statistical properties of both A_i and $B_{i,j}$ depend upon the time series data, from which X^tX is built, SVs temporally fluctuate for consecutive time series. Thus, the influence of dynamical noise on chaos can be extracted with a different form from that of measurement noise. This result means that the influences of dynamical noise and measurement noise can be distinguished even in the case of the noise-mixed data composed of both noises. The concrete way of extracting TFSV is explained next.

C. Estimation of TFSV

In practice, TFSV can be estimated as follows (see Fig. 1). First, temporally consecutive time series data sets are prepared. Each set is called an "*interval*" $\{I_k|k=1,2,\ldots,N_{int}\}$ in this paper. In each I_k, N elements are included such as $\{v_{N(k-1)},v_{N(k-1)+1},\ldots,v_{N(k-1)+N}\}$. Second, SVs $\{\sigma_k(i)|i=1,2,\ldots,n\}$ are obtained in each I_k, where i is an "*index*" of SVs lined in descending order. Third, the averaged SVs $\{a(i)|i=1,2,\ldots,n\}$ over all of I_k are calculated for every index such as $a(i)=1/N_{int}\Sigma_{k=1}^{N_{int}}\sigma_k(i)$. The difference between these two sets $\{\sigma_k(i)\}$ and $\{a(i)\}$ is regarded as the extent of TFSV; therefore, TFSV can be estimated by investigating this difference.

In order to determine the difference, we introduce a performance index: the correlation coefficient (C), which is obtained every I_k on the assumption that the system remains steady [19] (see also Fig. 1). Particularly, C_k for each I_k can be calculated as follows:

$$C_k=\frac{\sum_{i=1}^{n}(\sigma_k(i)-\overline{\sigma_k})(a(i)-\bar{a})}{\sqrt{\sum_{i=1}^{n}(\sigma_k(i)-\overline{\sigma_k})^2}\sqrt{\sum_{i=1}^{n}(a(i)-\bar{a})^2}}, \tag{3}$$

where $\bar{s}_k$ and $\bar{a}$ are the averages of $\sigma_k(i)$ and $a(i)$ for i, respectively, and $C_k\in[-1,1]$. As the difference between the sets $\{\sigma_k(i)\}$ and $\{a(i)\}$ becomes large, C_k becomes small, approaching 0 as it moves away from 1. However, in practice, the average of C_k; C_{av} is used as a proxy of C_k, so that we can grasp the whole tendency of all of C_k and TFSV can be estimated by C_{av}. Since a probability distribution of correlation coefficients is generally asymmetric, their average cannot be easily obtained. However, as the distribution can be transformed into a symmetric quasinormal one by means of Fisher's z transformation [20], C_{av} can be obtained by inversely transforming the arithmetic average at the quasinormal, obtained by Fisher's z transformation. A standard deviation can be also obtained from the quasinormal distribution in the same way, expressing numerical error.

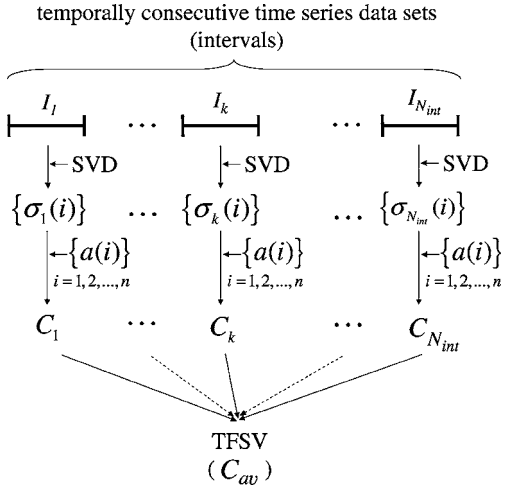

FIG. 1. The concept of the extraction of TFSV. Temporally consecutive time series data sets are prepared. Each of sets is called an "*interval*" $\{I_k|k=1,2,\ldots,N_{int}\}$. N elements; $\{v_{N(k-1)},v_{N(k-1)+1},\ldots,v_{N(k-1)+N}\}$ are included in each I_k. Meanwhile, each performance index C_k is calculated from the obtained SVs $\{\sigma_k(i)|i=1,2,\ldots,n\}$ in each I_k using the averaged SVs $\{a(i)|i=1,2,\ldots,n\}$. TFSV can be estimated by the average C_{av} as a proxy of C_k.

III. NUMERICAL ANALYSIS

A. Preparation

In the following section, Chua's electronic circuit is used as a typical chaos system, which is described by the three-dimensional ordinary differential equations that follow [21]:

$$C_1\frac{dV_{C_1}}{dt}=\frac{1}{R}(V_{C_2}-V_{C_1})-f_{N_R}(V_{C_1}), \tag{4a}$$

$$C_2\frac{dV_{C_2}}{dt}=\frac{1}{R}(V_{C_1}-V_{C_2})+i_L, \tag{4b}$$

$$L\frac{di_L}{dt}=-V_{C_2}, \tag{4c}$$

where $f_{N_R}(V_{C_1})=G_bV_{C_1}+\frac{1}{2}(G_a-G_b)|V_{C_1}+B_p|-|V_{C_1}-B_p|$. V_{C_1}, V_{C_2}, and i_L indicate voltage of two capacitors C_1, C_2,

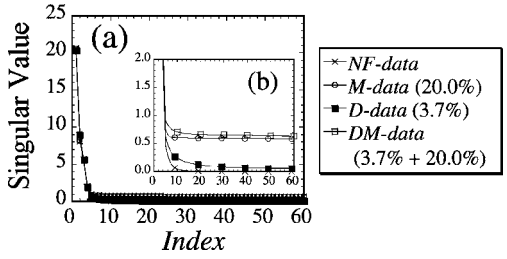

FIG. 2. Results of SVD with the (60,1) window of the four representatives in a certain I_k. As the first 4 SVs are relatively large for each of the cases, the number of leading SVs is 4, which is approximately equal to the original number 3 (a). The characteristic of measurement noise also appears in the uniform increase of all SVs as shown in the enlarged figure (b).

and the current of coil L, respectively; $f_{N_R}(V_{C_1})$ denotes the three-segment odd-symmetric voltage-current characteristic of the nonlinear resistor N_R, by which the system exhibits a large variety of typical chaotic behaviors. The *i.i.d.* dynamical noise ξ with a zero mean is added to V_{C_1} such that $V_{C_1} \rightarrow V_{C_1} + \xi$ as additive noise. In this work values of parameters giving rise to double-scroll chaos are selected as follows: $C_1 = 10$ nF, $C_2 = 100$ nF, $L = 18$ mH, $1/R = 0.55\ 1/\Omega$, $G_a = -0.758$ mA/V, $G_b = -0.409$ mA/V, and $B_p = 1.17$ V. Here, the analyses are performed for the scalar time series of V_{C_1}.

In this study, four kinds of time series are prepared, these being noise-free data (*NF*-data), measurement noise data (*M*-data), dynamical noise data (*D*-data), and noise-mixed data composed of both dynamical noise and measurement noise (*DM*-data). Each noise level is given as a ratio of a standard deviation of noise data to that of the time series V_{C_1} in *NF*-data. The range of the noise amplitude is 0.01%–20.0% for *M*-data and 0.01%–3.7% for *D*-data, where 3.7% is the maximum, below which a chaotic state can be retained. For *DM*-data, measurement noise with a 20.0% noise level is added to all *D*-data. The *fourth-order Runge-Kutta method* is used with a constant time step $\tau_s = 0.000\,005$. The number of elements N in each interval and the number of intervals N_{int} are 100 000 and 10 000, respectively. SVD is performed for all intervals to extract TFSV. However, ahead of SVD, an adequate (n,J) window should be determined, satisfying the window length $\tau_w = n\tau_L = nJ\tau_s$, where the lag time τ_L is expressed as $\tau_L = J\tau_s$. In particular, the most important parameter is τ_w. Though the detail is not presented here, in this case $\tau_w = 60\tau_s$ can be determined by considering the bandlimiting frequency in fast Fourier transform (FFT) analysis as explained in Ref. [17]. However, there are some difficulties in deciding the properties of the adequate window. This problem is still open to discussion, but the result should satisfy $nJ = 60$. Here, it is desirable to avoid the noise floor relevant to the nondeterministic basis in order to verify the essential behavior of the system as indicated in Refs. [17,22]. Accordingly, SVD is undertaken with a relatively larger $n = 60$, that is $(n,J) = (60,1)$ first in order to extract the number of the leading SVs.

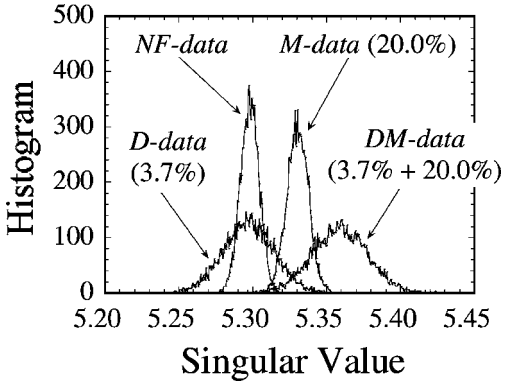

FIG. 3. Histograms of the same representatives in the first index. The shape of each histogram displays the extent of TFSV. As a lower and broader shape indicates a greater extent of TFSV, accordingly, the extent is larger in both *D*-data (3.7%) and *DM*-data (3.7% + 20.0%) from the shape of the histograms.

B. Results of SVD

Figure 2 shows results of SVD with the (60,1) window of the four representatives in a certain I_k, where SVs are arrayed in descending order. Here, in the case of *DM*-data, the percentages in parentheses indicate a dynamical and a measurement noise level, respectively. As the first 4 SVs are relatively large for each of the cases indicated in Fig. 2(a), it can be found that the number of leading SVs is 4, which is approximately equal to the original number 3. Accordingly, for the main analyses at the next stage, $n = 4$, that is $(n,J) = (4,15)$ is adopted. Here, the characteristic of measurement noise also appears in the uniform increase of all SVs as shown in the enlarged figure, Fig. 2(b). Next, TFSV is investigated for the first four leading SVs by using the (4,15) window. Results are expressed by histograms related to a frequency distribution of SVs. SVs calculated from all I_k are classified into four groups corresponding to the four indices and arranged in histograms with the interval width 5.5×10^{-5}. In Fig. 3 histograms of the same representatives in the first index are shown. The shape of each histogram displays the extent of TFSV. A lower and broader shape indicates a greater extent of TFSV. Accordingly, it can be observed that the extent is larger in both *D*-data (3.7%) and *DM*-data (3.7% + 20.0%) from the shape of the histograms. The same results are also obtained in all indices and in other noise levels. Meanwhile, the deviation in *NF*-data originates in numerical error.

C. Averaged correlation coefficient (C_{av})

In order to concretely obtain the features of histograms, C_{av} is calculated next. In Fig. 4 every C_{av} of *M*-data is nearly equal to that of *NF*-data independently of the noise amplitude, while each C_{av} of *D*-data and *DM*-data decreases as the noise level increases (a). Significant decreases can be seen especially above the approximately 1.0% noise level. It is inferred from the results that these changes correspond to the destruction of the structure of the system caused by dynamical noise. In addition, the influence in the noise-mixed data such as *DM*-data can also be discerned with both *NF*-data

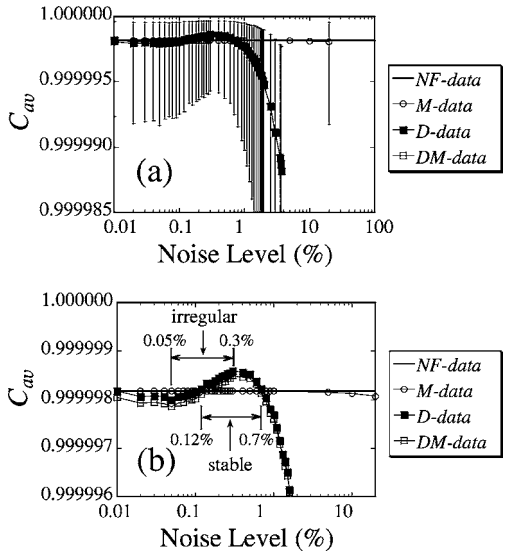

FIG. 4. C_{av} for all the data. The significant decrease can be seen above the approximately 1.0% noise level in C_{av} of *D*-data and *DM*-data, differently from those of *NF*-data and *M*-data (a). Here, error bars for *D*-data and *M*-data (20.0%) are partially indicated, while the irregular and the stable part can be seen in the middle noise levels around 0.05%–0.3% and 0.12%–0.7%, respectively, in the enlarged view (b). Error bars are abbreviated.

and *M*-data, independently of the noise amplitude. This result is the same as we expected before the analysis. Accordingly, in this study, we can discern from the enlarged view in Fig. 4(b) the influence of dynamical noise from that of measurement noise, especially at levels exceeding 0.02%, though this cannot be generalized. C_{av} in *D*-data and *DM*-data, however, also indicates temporarily and counterintuitively large values in the middle around 0.05%–0.3% as shown in the enlarged view, Fig. 4(b). We call this region an "*irregular part*." Furthermore, the C_{av} goes so far as to indicate a larger value than that of *NF*-data around 0.12%–0.7%. We call this region a "*stable part*." What happens in these regions will be discussed later.

Now, let us consider the dependence of C_{av} on the number of points N in each interval I_k. As illustrated in Fig. 5, related

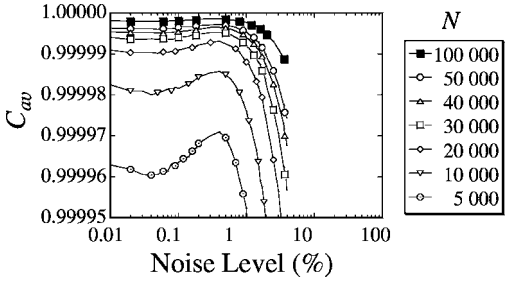

FIG. 5. Dependence of C_{av} on the number of points N in each interval I_k. In large N, C_{av} approaches 1, which corresponds to a noiseless instance, and the change of C_{av} becomes smaller. Particularly in the case of an extremely large N, numerical error cannot be ignored. In contrast, at an extremely small N, there is a statistical stability problem because of the extremely short number of points.

to *D*-data, if N becomes large, C_{av} approaches 1, which corresponds to a noiseless instance, and the change of C_{av} becomes smaller. Furthermore, C_{av} changes more smoothly against the change of the noise amplitude, because the difference of the statistical properties among the intervals decreases and, therefore, the influence of noise on the system cannot be identified. However, particularly in the case of an extremely large N, numerical error cannot be ignored, because the change of C_{av} becomes extremely smaller. Therefore, it becomes difficult to extract TFSV. Additionally, calculation time increases considerably. In contrast, in the case of an extremely small N, there is a statistical stability problem because of the extremely short number of points. Accordingly, an adequate N is required for extraction, though it is difficult to precisely determine the adequate value. In this work, the relatively large number 100 000 is selected to ensure reasonable calculation time and avoid the influence of numerical error.

IV. VERIFICATION OF VALIDITY

A. A flip-flop process

To verify the validity of our results, we focus on a flip-flop process, where a trajectory circulates away from the unstable fixed point on one lobe of a double-scroll attractor and switches to the other lobe after rotating several times, as explained in Ref. [10]. It can be maintained that dynamical noise affects the statistical features of the flip-flop process. Meanwhile, the flip-flop process can be described as a one-dimensional symbol sequence composed of 1 and 0. In a local maximum of V_{c1}, if a point of a trajectory is on one lobe of an unstable fixed point in a three-dimensional phase space and the maximum value of V_{c1} is positive, a symbol $s=1$ is assigned to the symbol sequence. Otherwise, such as in the case of a point on another lobe, an $s=0$ is assigned.

B. Shannon entropy

The influence of dynamical noise on the symbol sequence can be estimated by employing Shannon's familiar entropy measure. As the entropy describes an amount of information related to disorder of a system, it is expected to evaluate the amount of disorder of the system influenced by dynamical noise. According to Ref. [12], nth-order Shannon entropy H_n is based on the probability distribution of words of the length n in the symbol sequence as follows:

$$H_n = -\sum_{w^n \subseteq W^n, p(w^n)>0} p(w^n)\log_2 p(w^n), \tag{5}$$

where w^n denotes a word of the length n, W^n means the set of all of w^n, and $p(w^n)$ is the probability that w^n appears in the symbol sequence. Here, the *Shannon entropy difference* h_n is obtained from H_n as follows:

$$h_n = H_{n+1} - H_n, \tag{6a}$$

$$h_0 = H_1, \tag{6b}$$

where h_n describes the mean information quantity for a symbol sequence. Each h_n with $n \geqslant p$ vanishes for period p se-

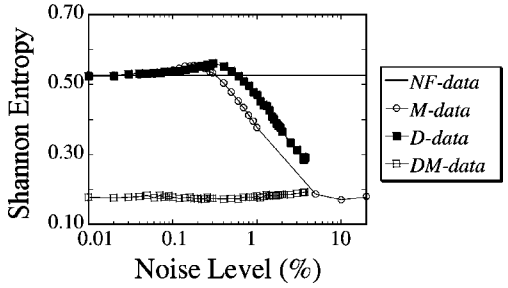

FIG. 6. Shannon entropy for all the data. At least two obviously irrational problems can be seen. One is that the entropy of *M*-data and *D*-data counterintuitively indicates much smaller values at large noise levels. The other is that the entropy of *DM*-data is lower than those of any other types of data, in spite of the presence of large measurement noise (the noise level is 20%).

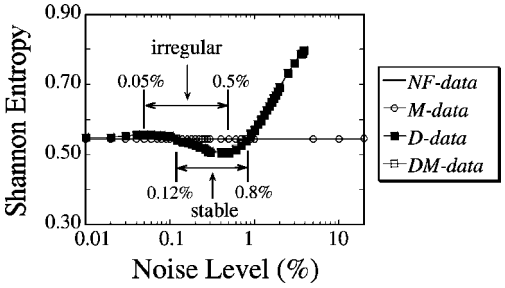

FIG. 7. Shannon entropy for the coarse-grained trajectories in all the data. The entropy correlates highly with C_{av} in regard to all of the data. The quite similar counterintuitive behavior to that of C_{av} is also observed at the irregular part (around 0.05%–0.5%) and the stable part (around 0.12%–0.8%).

quences and, on the other hand, each h_n is equal to n for a purely random symbol sequence. Accordingly, the entropy h can be expressed as the limit of h_n as follows:

$$h = \lim_{n\to\infty} h_n. \tag{7}$$

In this study, the statistical features of the flip-flop process can be sufficiently investigated by knowing the change of the entropy around the typical time scale of the switching processes as referenced in Ref. [13]. This typical time scale can be regarded as the mean passage time 5.1 when the trajectory passes on the same lobe in *NF*-data. Accordingly, $n=5$ can be determined. The entropy h is defined as h_5. If the disorder of the flip-flop process increases, h_5 becomes large. In contrast, if the disorder decreases and a stable state arises, h_5 becomes small. The results of the entropy are shown in Fig. 6. Here, the number of points in each symbol sequence is 100 000. From this figure, at least two obviously irrational problems arise. One is that the entropy of *M*-data and *D*-data counterintuitively indicates much smaller values at large noise levels. The other is that the entropy of *DM*-data is lower than those of any other types of data, in spite of the presence of large measurement noise (the noise level is 20%). The reason behind these problems is that numerous local maximum points, irrelevant to a flip-flop process, are generated by a large noise; therefore, the frequencies of words with the longer constant sequence, such as "11111," "00000," "11110," "01111," and so on, increase and, consequently, apparent stable states seem to occur, though such states are not practically produced as the flip-flop process.

C. Shannon entropy for coarse-grained trajectory

To avoid these problems, smoothing is utilized prior to the extraction of the symbol sequences. In this study, a moving average operation with 20 time steps is introduced as a smoothing method, and the coarse-grained trajectories are obtained with the small fluctuations fully eliminated from the original trajectories. After the extraction of the symbol sequences from the coarse-grained trajectories, Shannon entropy is calculated for the sequences. The results of the entropy are shown in Fig. 7.

The entropy of *M*-data is relatively stable against the increase of the noise amplitude. Behaving quite differently from that of *M*-data, each entropy of *D*-data and *DM*-data increases on the whole as the noise amplitude increases. An especially significant increase can be seen above the noise level of approximately 1.0%. These results are quite similar to those of C_{av}. From these results, it can be found that the striking change observed in C_{av} above the approximately 1.0% noise level originates in the disorder of the system, presumably due to the destruction of the system structure caused by dynamical noise as mentioned before. Furthermore, the irregular part (around 0.05%–0.5%) where the entropy counterintuitively decreases, and the stable part

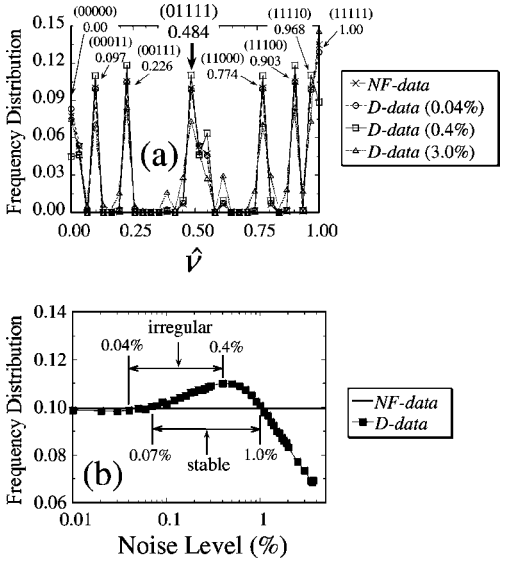

FIG. 8. Frequency distributions of all the words of the length 5. Changes in the distribution are dependent on $\hat{\nu}$ in any data. The similar behavior to a period of approximately 5 in the flip-flop process originally arises in the main (a). The striking similarity in appearance with both C_{av} and the entropy can be identified by the common tendency against a noise amplitude increases and the manifest inclusion of the counterintuitive change in both the irregular part (around 0.04%–0.4%) and the stable part (around 0.07%–1.0%) in the case of the decimal word $\hat{\nu}=0.484$ corresponding to a binary word "01111" in (a) (b).

(around 0.12%–0.8%) where the values are lower than those of *NF*-data can be seen. From the results, the entropy correlates highly with C_{av} even in these parts in regard to all of the data. Accordingly, it can be surmised that the counterintuitive behaviors observed in both C_{av} and the entropy probably indicate the transition of the system to the stable states similar to period p ($p \leqslant 5$) and are essential to the system. Consequently, it can be found, from the results of the traditional Shannon entropy measure, that C_{av} allows us to extract the complexity caused by dynamical noise. Next, the counterintuitive behavior in the irregular and the stable parts is examined.

D. Noise-induced stabilization

Frequency distributions of all the words are investigated, so that we can see how a pattern of the flip-flop process changes depending on a noise amplitude [10]. In Fig. 8, frequency distributions of all the words of the length 5 are shown for *NF*-data and *D*-data, with four noise levels as representatives. Each binary word can be transformed into a corresponding decimal word as follows:

$$s_k s_{k+1} \cdots s_{k+n-1} \rightarrow \nu = \sum_{k=1}^{n} s_k \times 2^{k-1}, \tag{8}$$

where s_k is a kth symbol on the symbol sequence, and $s_k s_{k+1} \cdots s_{k+n-1}$ and ν are a binary and a decimal word, respectively, as explained in Ref. [10]. Here, ν is normalized as $\hat{\nu} = \nu/(2^n - 1)$. Based on Fig. 8(a), it can be shown that changes in the distribution are dependent on $\hat{\nu}$ in any data and, in addition, some of $\hat{\nu}$ indicating large peaks correspond to words of longer constant sequences, such as "11111," "00000," "11110," "01111," and so on. Particularly, as the existence of the large peaks corresponding to "11111" and "00000" means that the similar motion to period approximately 5 in the flip-flop process orginally arises in main. Here, some peaks of relatively shorter constant sequences "11100", "00011", "11000", and "00111", which are also illustrated in this Fig. 8(a), inevitably exist in the presence of the longer constant sequences "11111", "00000", "11110", and "01111". Accordingly, the existence of such shorter sequences does not necessarily imply peroid 2 or 3. At every $\hat{\nu}$, as the value of each peak depends on a noise level, the behavior of the flip-flop process depends on the noise amplitude. The appearance is expressed in Fig. 8(b). This shows the result in the case of the decimal word $\hat{\nu} = 0.484$ corresponding to a binary word "01111" as indicated in Fig. 8(a). According to this figure, the striking similarity in appearance with both C_{av} and the entropy can be identified by the common tendency against a noise amplitude increases and the manifest inclusion of the counterintuitive change in both the irregular part (around 0.04%–0.4%) and the stable part (around 0.07%–1.0%). Furthermore, the ranges of these parts correspond closely with those of C_{av} and the entropy. Additionally, from Fig. 8(a), it can be found that in *D*-data (0.4%), which indicates the maximum frequency distribution in Fig. 8(b), the frequency distributions at 1.00 and 0.00 corresponding to "11111" and "00000" associated with the periodic motion of period 5 decrease and, instead, those of the decimal words corresponding to "11110," "01111," "11100," "00011," "11000," "00111," and so on associated with the periodic motion of period 4 increase. Consequently, the dominant period changes from approximately 5 to approximately 4 due to the noise, and the periodic stable behavior is emphasized. At this state, C_{av} indicates a large value approaching 1, since the fluctuation of the singular values becomes small, while Shannon entropy decreases, as the disorder of the flip-flop process decreases and a periodic behavior is emphasized. More specifically, noise-induced stabilization such as coherence resonance is generated as indicated in Refs. [9–11]. Further detailed investigation is required to ascertain the mechanism of the noise-induced stabilization.

Quite similar results are obtained from C_{av}, Shannon entropy, and frequency distribution, there are differences between our method compared with the others. In the cases of entropy and frequency distribution, it is necessary to smooth the original time series data and extract the symbol sequence from it prior to the analysis, as explained in Sec. IV. This is disadvantageous due to the increased number of processes, the increased possibility of error resulting from the additional operations, the increased complexity of the operation, and the like. Our method determines the difference between the influence of dynamical noise and that of measurement noise without any preprocessing. Accordingly, our method is particularly robust for the analysis of real-world data, where both dynamical noise and measurement noise are present. The proposed method has already been applied to other types of noise, including additive noise with a uniform probability distribution and multiplicative noise with a Gaussian and a uniform one. Qualitatively similar results to the aforementioned have been obtained in any case. In addition, though the details are not presented here, the validity and the effectiveness of this method was verified and confirmed with the Lorenz system in another typical chaotic system.

V. CONCLUSIONS

The influence of dynamical noise on chaos can be numerically extracted by using the proposed method even in the presence of measurement noise. The extraction is performed by detecting the temporal fluctuation of singular values obtained from SVD. From the results, it can be shown that, as expected, changes of C_{av} are dependent on noise amplitude. The results of C_{av} are quite similar to those derived using Shannon entropy and frequency distribution. Accordingly, it can be said that C_{av} allows us to extract the complexity stem from the destruction of the system structure and the generation of stable states caused by dynamical noise. Counterintuitive behaviors are observed in any method. In this instance, these behaviors probably are essential to the system, and indicate the transition of the system to the stable states from the results of frequency distribution. Although quite similar results are obtained from C_{av}, Shannon entropy, and frequency distribution, there are some differences in our method in comparison with the other methods. In the cases

of entropy and frequency distribution, it is necessary to smooth the original time series data and extract the symbol sequence prior to the analysis. This is disadvantageous due to the increased number of processes, the increased possibility of error caused by the additional operations, the increased complexity of the operation, and so on. Our method can determine the difference between the influence of dynamical noise and that of measurement noise without any preprocessing. Accordingly, it can be said that our method is particularly robust for the analysis of real-world data, where both dynamical noise and measurement noise are present. Analyses are shown only for the case of Chua's electronic circuit. However, our method has already been applied to other types of noise, and qualitatively similar results to the aforementioned have been obtained in any case. In addition, though the details are not presented here, the validity and the effectiveness of our method was verified and confirmed in another typical chaotic system using the Lorenz system.

ACKNOWLEDGMENTS

We would like to thank Professor K. Aihara of the University of Tokyo for his fruitful comments and Professor T. Ikeguchi of Saitama University for stimulating discussions and for his useful comments. This research was supported by a Grant-in-Aid for Scientific Research of JSPS.

[1] M. E. Davies, Chaos **8**, 775 (1998).
[2] J. P. M. Heald and J. Stark, Phys. Rev. Lett. **84**, 2366 (2000).
[3] C. L. Bremer and D. T. Kaplan, Physica D **160**, 116 (2001).
[4] L. Gammaitoni, P. Hänggi, P. Jung, and F. Marchesoni, Rev. Mod. Phys. **70**, 223 (1998).
[5] A. A. Zaikin, K. Murali, and J. Kurths, Phys. Rev. E **63**, 020103 (2001).
[6] P. S. Landa and P. V. E. McClintock, J. Phys. A **33**, L433 (2000).
[7] A. A. Zaikin, L. López, J. P. Baltanás, J. Kurths, and M. A. F. Sanjuán, Phys. Rev. E **66**, 011106 (2002).
[8] J. P. Baltanás, L. López, I. I. Blechman, P. S. Landa, A. A. Zaikin, J. Kurths, and M. A. F. Sanjuán, Phys. Rev. E **67**, 066119 (2003).
[9] A. S. Pikovsky and J. Kurths, Phys. Rev. Lett. **78**, 775 (1997).
[10] R. Wackerbauer, Phys. Rev. E **52**, 4745 (1995).
[11] E. I. Volkov, M. N. Stolyarov, A. A. Zaikin, and J. Kurths, Phys. Rev. E **67**, 066202 (2003).
[12] A. Witt, A. Neiman, and J. Kurths, Phys. Rev. E **55**, 5050 (1997).
[13] R. Wackerbauer, Phys. Rev. E **58**, 3036 (1998).
[14] R. Wackerbauer, Phys. Rev. E **59**, 2872 (1999).
[15] P. S. Landa, A. A. Zaikin, V. G. Ushakov, and J. Kurths, Phys. Rev. E **61**, 4809 (2000).
[16] J. B. Gao, W.-W. Tung, and N. Rao, Phys. Rev. Lett. **89**, 254101 (2002).
[17] D. S. Broomhead and G. P. King, Physica D **20**, 217 (1986).
[18] E. J. Kostelich and T. Schreiber, Phys. Rev. E **48**, 1752 (1993).
[19] T. Ikeguchi and K. Aihara, IEICE Trans. Fundamentals **E78-A**, 1291 (1997).
[20] R. A. Fisher, Biometrika **10**, 507 (1915).
[21] R. N. Madan, *World Scientific Series on Nonlinear Science Ser. B-1, Chua's Circuit: A Paradigm for Chaos* (World Scientific, Singapore, 1993).
[22] A. M. Fraser, Physica D **34**, 391 (1989).